



## Definition and dynamic portrait of large space structures for control system synthesis

V.J. Rutkovsky,<sup>a</sup> V.M. Sukhanov,<sup>a</sup> S.J. Dodds<sup>b</sup>

<sup>a</sup>*Institute of Control Sciences of the Russian Academy of Sciences, Profsoyuznaya 65, 117806, Moscow, Russia*

<sup>b</sup>*Department of Electrical and Electronic Engineering, University of East London, Longbridge Road, Dagenham, Essex RM8 2AS, UK*

### Abstract

A new definition of large space structures (LSS) is given, yielding a mathematical model of minimal order for three-axis attitude control system synthesis. Then, the dynamic portrait is introduced, allowing the structure to be designed with minimal excitation of certain vibration modes by the control variables. The theory is developed by considering space structures having a branched configuration near the centre of which are located attitude sensors and actuators collocated with an orthogonal control axis set to be orientated. It is well known that the complete set of space structures comprises two subsets, one in which rigid body dynamics may be assumed and the other, referred to as the Large Space Structures (LSS), for which one or more flexure modes, typically with very low natural frequencies, must be taken into account. This paper provides a much needed quantitative boundary between the two subsets, given by the definition that a structure is a LSS if the inequalities,  $k_i > 2.47$  and  $\omega_i^2 < 2k_i$ , are satisfied for any  $i$ , where  $\omega_i$  and  $k_i$  are, respectively, the natural frequency and excitability coefficient of the  $i^{\text{th}}$  flexure mode. The approach is based on a comparison of the flexure mode motion with the rigid-body mode motion in the phase double-plane ( $i^{\text{th}}$  modal phase-plane superposed on the rigid-body phase-plane) of a structural model in the modal state representation to which is applied a step control variable. Hence, the model derived is suitable for designing control systems employing discontinuous on-off thrusters as well as continuous actuators. The Lagrangian and Modal dynamic models of the structure are then used together to derive the dynamic portrait as a set of



graphs,  $[\omega_i](\lambda)$  and  $[k_i](\lambda)$ , where  $\lambda$  is a selected physical parameter of the spacecraft. The structure may be designed, where practicable, to correspond with minima in these graphs to simplify the control problem. The new method is demonstrated by examples.

## 1 Introduction

A new approach is presented for obtaining a mathematical model of the dynamics of large structures in space on which the synthesis of three-axis attitude control laws may be based. The method presented here concentrates on the many space structures requiring attitude control which have a branched configuration at the centre of which is located an orthogonal control axis set to be orientated by automatic control, the attitude sensors and actuators being collocated with this control axis set. This restricted class of space structures will be referred to as spacecraft. Attention is focussed on a subset of the set of spacecraft, referred to as Large Flexible Spacecraft (LFS) having flexure modes with very low frequencies, referred to as significant modes, which pose the most challenging problems to the control system designer. This paper introduces a rigorous definition of LFS via the identification of a quantitative boundary for the segregation of LFS from the complete set of spacecraft. The approach, which is suited to control systems employing discontinuous thrusters as well as continuous torque actuators, is introduced here via the simplified model of such spacecraft in which inter-axis coupling is negligible, starting with the Lagrange equations:

$$J\ddot{x} + \sum_{i=1}^M a_i q_i = \Gamma, \quad a_i \ddot{x} + \sum_{j=1}^M (\tilde{J}_j \ddot{q}_j + b_j q_j), \quad i = 1, 2, \dots, M$$

where  $x$  is any Euler angle, i.e., the attitude angle to be controlled,  $q_i$  are generalised co-ordinates,  $J, \tilde{J}_i, a_i$  and  $b_i$  are constant parameters of the spacecraft, to be defined in the following section, and  $\Gamma$  is the control torque. Next, this model is transformed into the modal form as given by Nurr et. al. [1]:-

$$\ddot{\bar{x}} = u, \quad u = \Gamma/J, \quad \ddot{\bar{x}}_i + \omega_i^2 \bar{x}_i = k_i u, \quad i = 1, 2, \dots, M, \quad x = \bar{x} + \tilde{x}, \quad \tilde{x} = \sum_{j=1}^M \tilde{x}_j$$

where  $\bar{x}$  is the attitude angle which would result if the whole structure moved as a rigid body under the same control torque, i.e., the mean value of the true attitude angle,  $x$  and  $\tilde{x}$  is the additional deflection resulting from the deflections,  $\tilde{x}_i$ , of the individual flexure modes. The constant dynamic

parameters are now the vectors of fundamental frequencies,  $\omega = [\omega_i]$ , and excitability coefficients  $\mathbf{k} = [k_i]$  which are directly relevant to attitude control system synthesis.

The aforementioned quantitative boundary for the segregation of LFS from the set of spacecraft is derived using the double-phase plane method of Rutkovsky and Sukhanov[2][3] in which the origin of the motion of  $[\tilde{x}_i, \dot{\tilde{x}}_i]$  in the modal phase plane is centred on  $[x, \dot{x}]$  of the rigid-body mode phase plane. The method is based on a comparison of the phase trajectories (i.e., state trajectories) of the rigid-body mode and the flexure modes. The result, derived in section 5, is that a LFS is defined by the conditions,  $k_d > 2.47$  and  $\omega_d^2 < 2k_d$  where  $d$  is the index of the dominant mode.

From the Lagrangian and Modal spacecraft models, a relationship of the form,  $f(J, J_i, a_i, b_i, [\omega_i], [k_i])$ , follows from which a set of graphs,  $[\omega_i](\lambda)$  and  $[k_i](\lambda)$ , is derived, where  $\lambda$  is any physical dynamics parameter of the spacecraft. This set of graphs constitutes the *dynamic portrait* of the LFS, which facilitates model order reduction. Also, there are minima in the graphs for certain values of  $\lambda$ , rendering the dynamic portrait useful for optimisation of the spacecraft structural design to ease the control problem.

## 2 Generic Mathematical Model of Spacecraft

### 2.1 Basis of Model Formulation

To commence the model development, the following definition of large flexible spacecraft (LFS) given by Nurr, et. Al., [1] and by several contributors in Kirk [4] is first considered:-

A flexible spacecraft is a LFS if it has physically large dimensions and if the spectral band of elastic oscillation frequencies in the structure overlaps or is close to the spectral band of the ideal controlled motion of the spacecraft as a rigid body.

Clearly, under these circumstances, the flexure modes of the structure must be taken into account in the attitude control system design and this gives the definition some practical meaning.

It is important to note that if the lowest elastic oscillation frequency is very low ( $f_{\min} < 0.5$  [Hz], say), then the natural damping is very poor. This is true because the damping ratios of typical space structures are usually of the order of  $\zeta = 10^{-3}$  and the time constant of decay of the oscillation magnitude of the



lowest frequency mode is  $T_{\max} = 1/(2\pi\zeta f_{\min}) > 318$  [s] which is excessive. This calls for control laws capable of providing active modal damping and these generally can only be designed using a model including the significant modes.

A limitation of the above definition, however, must now be pointed out. It is well known that the closure of a control loop around any dynamical system, changes its dynamic characteristics and so the frequencies of the flexure modes depend not only on the physical structure of the spacecraft but also on the particular attitude control system employed. This creates a difficulty in using the aforementioned definition which refers only to the 'open loop' system. A precise definition of LFS is developed here which overcomes this difficulty.

In order to develop a generic spacecraft model, a generalised mechanical construction must be chosen for which the equations of motion can be derived. A wide variety of FS configurations, however, result from different mission requirements and these must be catered for. Nevertheless, this large variety of mechanical configurations can be grouped into three basic categories:-

- i) FS with continuous mass distribution which are modelled by partial differential equations.
- ii) FS comprising a rigid centre-body to which is attached one or more elastic appendages with distributed parameters.
- iii) FS which can be regarded as a rigid centre-body to which is attached a number of appendages, each regarded as a chain of other rigid bodies connected via massless elastic links.

Attempting to use the partial differential equations appropriate to category (i) directly for the analysis and design of practicable control systems leads to insurmountable obstacles as reported by Lurye[5]. The mathematical model for category (ii) is based on the well known method of hybrid co-ordinates and comprises a mixed set of ordinary and partial differential equations, but again this is not practicable for control system synthesis. Category (iii) is the most common and may be modelled by ordinary differential equations in terms of a set of generalised co-ordinates, the number of which is determined by the spacecraft configuration. This, being a model of finite order, lends itself readily to control system synthesis. It is well known, that a mechanical dynamical system with distributed parameters can be represented by a lumped parameter model of finite order to a certain accuracy. This means that category (i) and (ii) spacecraft can ultimately be represented as category (iii) spacecraft. Hence, the generic model developed here refers to category (iii). In view of its general shape, category (iii) spacecraft are described as having a *branched* configuration.

Typical appendages of branched LFS are elastic solar panels, large deployable antennas (sometimes with actuators) and docked transportation modules in the case of space stations. All these elements can be divided into two groups:-

- 1) Elastic plates (representing, for example, solar panels and antenna reflectors).

2) Rigid bodies, which are connected to the rigid centre-body by massless elastic links.

In addition to this, it is necessary to take into consideration additional degrees of freedom of relative motion such as associated with pointing mechanisms for antennae and solar panels. Thus, the spacecraft model must, in general, be time varying.

The *generalised mechanical structure* of LFS on which the generic mathematical model is based is a branched structure comprising a rigid centre-body with an arbitrary, finite number of flexible appendages in both groups (1) and (2). This is considered to be sufficient for most practical purposes. For example, FS SAT 2 referred to in Kirk[2] and Ekran studied by Nekhoroshiy et. al.[7] are LFS that are well represented by such a model structure. Figure 1 shows the common appearance of the generalised mechanical structure.

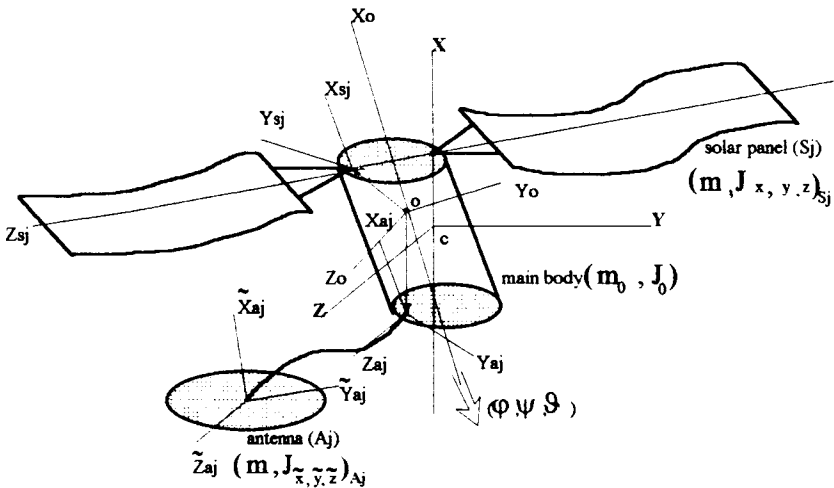


Figure 1 A spacecraft represented within the generalised structure framework

To reduce the mathematical model to minimal order in a form suitable for attitude control system synthesis, it is necessary to convert the elastic elements' models of group (i) to finite order models. This is achieved here by finding the minimal number of mass points,  $r$ , of the original distributed system allowing motion approximating the mode shapes that are known to exist and affect the centre-body attitude. Three main conditions of dynamic equivalence between the original and simplified systems must be satisfied in this process:-

C1) The condition of mass equality:- 
$$\int_S m ds = \sum_{k=1}^r m_k = m_S$$

C2) The condition of reduced moment of inertia equality:- 
$$\int_S m \rho^2 ds = \sum_{k=1}^r m_k \rho_k^2 = J_{x,y,z}$$



C3) The condition of fundamental frequency coincidence (or nearness) of the finite-dimensional model and the original elastic element.

Condition C3 requires further explanation. Figure 2 shows a type (1) elastic element, exemplified as a solar panel, together with its lumped parameter model.

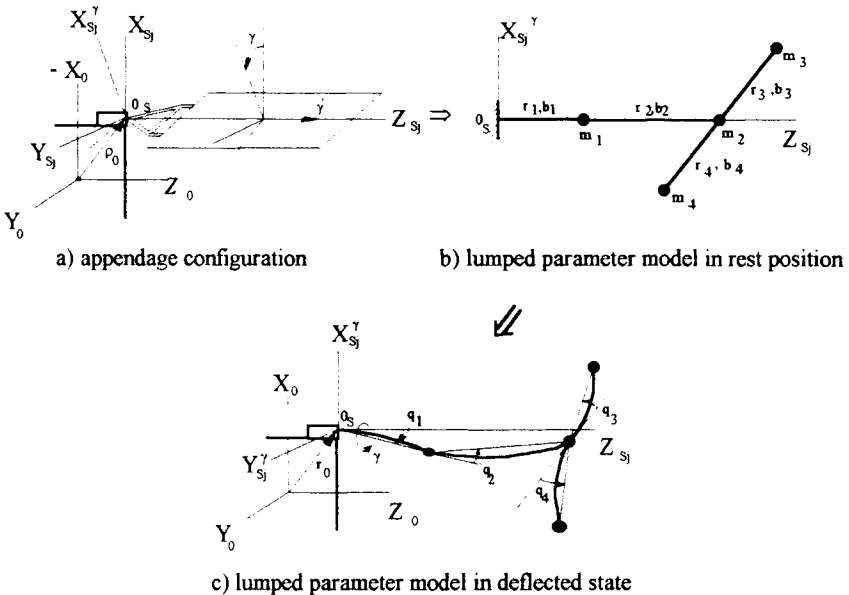


Figure 2 Formation of a lumped parameter model of a flexible appendage

The finite-dimensional model with  $r = 4$  reflects the main mode shapes of the oscillations (longitudinal, transverse and torsional) of the original flexible appendage of Figure 2(a). The parameters of the finite order model,  $m_i, r_i, b_i$ , are, respectively, the mass, length and spring constant of the  $i^{th}$  link.

As the solar panel is rotated relative to rigid centre-body of the spacecraft (to maintain solar power output) through the angle,  $\gamma$ , then the planes of the flexure mode oscillations are rotated by the same angle with respect to the control axes, thereby changing the dynamic characteristics.

With the generalised co-ordinates,  $q_s = (q_1, \dots, q_4, \gamma)$ , of Figure 2, where  $\gamma = \bar{\gamma} + \tilde{\gamma}$ ,  $\bar{\gamma}$  and  $\tilde{\gamma}$  being, respectively, the nominal solar panel orientation angle and the torsional oscillation component of the solar panel root where it joins the main body, the following expressions for the potential and kinetic energies of the finite order model may be derived for the  $j^{th}$  panel:-

$$P_{S_j} = \frac{6b_1b_2}{4b_1 + 21b_2} \left[ \left( \frac{b_i}{b_2} + 1 \right) q_1^2 + q_2^2 - q_1q_2 \right] + \frac{3}{2} (b_3q_3^2 + b_4q_4^2) + \frac{1}{2} C_\gamma \tilde{\gamma}^2$$

where  $b_1 = \frac{B_1}{r_1}$  and  $C_\gamma$  are the reduced bending and torsional spring constants.

$$K_{S_j} = \frac{1}{2} \left[ \begin{aligned} & m_1 r_1^2 \dot{q}_1^2 + m_2 (l\dot{q}_1 + r_2 \dot{q}_2)^2 \\ & + m_3 (l\dot{q}_1 + r_2 \dot{q}_2 + r_3 (\dot{q}_3 + \dot{\gamma}))^2 + m_4 (l\dot{q}_1 + r_2 \dot{q}_2 + r_4 (\dot{q}_4 + \dot{\gamma}))^2 \end{aligned} \right]$$

where  $l = r_1 + r_2$ . These expressions may then be used in Lagrange's formulation to determine the system of equations governing the oscillations of the solar panel, provided they are of sufficiently small amplitude for the assumption of linear springs to hold. Furthermore the equation for the fundamental frequencies follows in the form,  $\Delta(\tilde{\Omega}^2) = 0$ , the solution of which yields  $r$  functions  $\tilde{\Omega}_i^2 = F_i(\lambda)$ ,  $i = 1, \dots, r$ , expressing the dependence of the fundamental frequencies on the parameter vector  $\lambda = (m_1, \dots, m_4, r_1, \dots, r_4, b_1, \dots, b_4, C_\gamma)_j$ . If  $\tilde{\Omega}_{i0}$  are the fundamental frequencies of the original *distributed* model of the solar panel then if  $F_i(\lambda) = \tilde{\Omega}_{i0}^2$ ,  $i = 1, \dots, r$ , then the task of deriving the equivalent finite-dimensional model of the type (1) elastic element will have been solved.

Elastic elements of the second type already have a finite-dimensional structure the mass distribution of the elastic link being neglected. The expression for the potential energy of an elastic link on the top of which there is an additional body  $A_j$ , as illustrated in Figure 3, may be determined using the method of Lurye[5] and is as follows:-

$$P_{A_j} = \left[ \frac{6B}{r_A^3} \left( q_x^2 + \frac{r}{3} \phi_x^2 - \frac{r^2}{2} q_x \phi_x + q_y^2 + \frac{r}{3} \phi_y^2 - \frac{r^2}{2} q_y \phi_y \right) + \frac{2C_A}{r_A} \phi_z^2 \right]_{A_j}$$

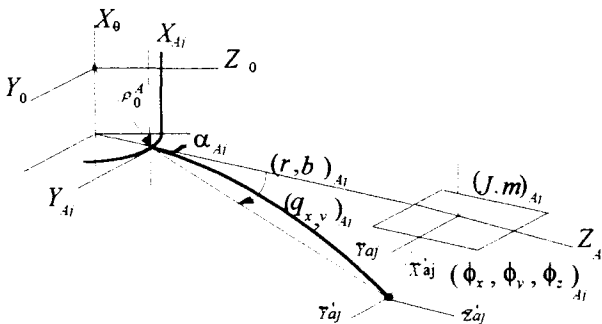


Figure 3 Geometry of deflected link interconnection

where  $B_{A_j}$  and  $C_{A_j}$  are the bending and torsional spring constants of link  $r_{A_j}$  with elastic displacement co-ordinates  $(q_x, q_y, \phi_x, \phi_y, \phi_z)_{A_j}$ .

Figure 4 illustrates the generalised lumped parameter FS model with generalised co-ordinates,  $q = (q_0, q_-)$ .

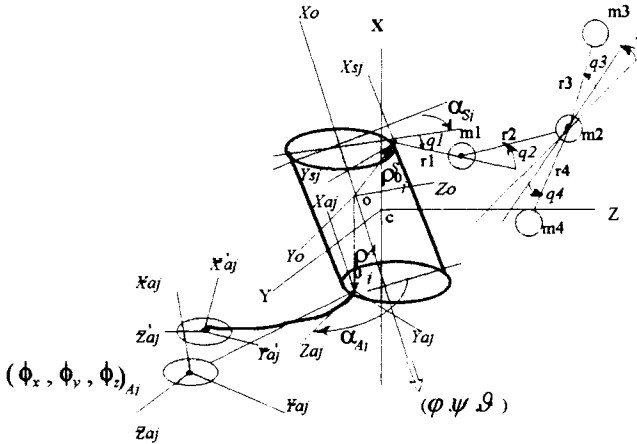


Figure 4 Geometric illustration of generic spacecraft model

The sub-vector,  $q_0 = (\varphi, \psi, \vartheta, \rho_{oc})$ , defines the location,  $\rho_{oc}$ , of the main body centre of mass,  $c$ , and its orientation in terms of the Euler angles  $(\varphi, \psi, \vartheta)$  with respect to the base co-ordinate system  $cXYZ$ . The sub-vector,  $q_- = (q_S, q_A)$ , defines the instantaneous elastic deformation of the spacecraft. The elastic part of the spacecraft comprises the solar panels,  $N_S$ , with elastic deformation co-ordinates,  $q_S = (\gamma, q_1, \dots, q_4)_{S_j}$ , as previously defined, together with an antenna platform,  $N_A$ , connected to the main body by elastic links, with elastic deformation co-ordinates,  $q_A = (q_x, q_y, \phi_x, \phi_y, \phi_z)_{A_j}$ . In addition, the position vectors of the attachment points of the flexible appendages to the main body are denoted by  $\rho_{0j}^S, \rho_{0j}^A = (m_0, J_{0x,y,z}), (r_{1,\dots,4}, m_{1,\dots,4}, B_{1,\dots,4})_{j_S}$  and  $(r, B, m, J_{\bar{x}, \bar{y}, \bar{z}})_{j_A}$ ,  $j_S = 1, \dots, N_S$ ,  $j_A = 1, \dots, N_A$ , are the mechanical and geometric parameters of the main and additional bodies of the FS. In this notation, the suffices,  $j_S$  and  $j_A$ , are ascribed to every element inside the parenthesis. For example,  $(\gamma, q_1)_{j_S} \equiv (\gamma_{j_S}, q_{1j_S})$ .

It must be noted that the lumped parameter model, as developed so far, allows only four flexure modes per flexible appendage and if more than this is required, the same principles would have to be applied with more mass points.



This would achieve the original objective of deriving a lumped parameter solar panel model with an arbitrary set of flexure modes.

Recalling that the solar panel rotation angle,  $\gamma$ , comprises two components,  $\bar{\gamma}$  and  $\tilde{\gamma}$ , it should be noted that the mean angle,  $\bar{\gamma}$ , generally varies far more slowly than the oscillatory component,  $\tilde{\gamma}$ , so that  $\dot{\gamma} \cong \dot{\tilde{\gamma}}$ . Also, the oscillatory component of the angle is assumed to be much less than the mean value so that  $\sin(\gamma) \cong \sin(\bar{\gamma})$ ,  $\bar{\gamma} \in (0 - 2\pi)$ .

## 2.2 Derivation of Model Equations

Lagrange's equation:-

$$\frac{d}{dt} \frac{\partial L}{\partial \dot{q}_i} - \frac{\partial L}{\partial q_i} = F_i \quad (1)$$

forms the basis of the mathematical model represented geometrically in Figure 3, where  $L = K(\dot{q}_i, q_i) - P(q_i)$ ,  $i = 1, \dots, n+3$  is the Lagrangian,  $K(\dot{q}_i, q_i)$  and  $P(q_i)$  are, respectively, the kinetic and potential energies of the complete spacecraft and  $F_i$  is the  $i^{\text{th}}$  generalised force. Note that this is truly a *force* if the co-ordinate,  $q_i$ , is a *translational* displacement, but is a *torque* if  $q_i$  is an *angular* displacement. Dimensional analysis (in SI units) of equation (1) agrees with this.

These equations yield many non-linear terms such as gyroscopic cross-coupling torques and coriolis forces, but these are found to be insignificant compared with the linearly occurring inertial forces and torques in most spacecraft applications. With this assumption, Likins[6] has derived the following linear differential equations for the three-axis angular motion of FS using Lagrange's method and then omitting the non-linear terms:-

$$\mathbf{J}\ddot{\mathbf{q}}_0 + \mathbf{A}_m \ddot{\mathbf{q}}_{\sim} = \Gamma, \quad \mathbf{A}_m^T \ddot{\mathbf{q}}_0 + \mathbf{J}_{\sim} \ddot{\mathbf{q}}_{\sim} + \mathbf{B}_{\sim} \mathbf{q}_{\sim} = 0 \quad (2)$$

where  $\mathbf{J}$  is the  $(3 \times 3)$  inertia tensor (sometimes referred to as the inertia matrix) applicable to the non-deformed spacecraft,  $\mathbf{A}_m$  is the  $(3 \times n)$  mass-inertia coefficient matrix determining the interaction between the FS's elastic parts and the rigid centre-body,  $\mathbf{J}_{\sim}$  is the  $(n \times n)$  characteristic inertia matrix of the elastic part of the FS,  $\mathbf{B}_{\sim}$  is the  $(n \times n)$  rigidity matrix of elastic elements (i.e., the matrix of spring constants of the elastic links between the mass elements of the flexible part).  $\Gamma = [\Gamma_X \ \Gamma_Y \ \Gamma_Z]^T$  is the control torque (or moment) vector applied to the rigid centre-body. As previously stated, the natural damping of flexure modes in space structures is usually negligible and so the model of



equations (2) does not include such damping which is evident through terms involving the velocity vector,  $\dot{\mathbf{q}}$ , being absent.

For use in a simulation programme, the component scalar differential equations of the mathematical model are needed. These may be obtained as the component equations of the following combined form of equations (2):-

$$\begin{bmatrix} \mathbf{J} & \mathbf{A}_m \\ \mathbf{A}_m^T & \mathbf{J}_\sim \end{bmatrix} \begin{bmatrix} \ddot{\mathbf{q}}_0 \\ \ddot{\mathbf{q}}_\sim \end{bmatrix} + \begin{bmatrix} \mathbf{0} & \mathbf{0} \\ \mathbf{0} & \mathbf{B}_\sim \end{bmatrix} \begin{bmatrix} \mathbf{q}_0 \\ \mathbf{q}_\sim \end{bmatrix} = \begin{bmatrix} \mathbf{I} \\ \mathbf{0} \end{bmatrix} \Gamma$$

i.e.,

$$\mathbf{A}\ddot{\mathbf{q}} + \mathbf{B}\dot{\mathbf{q}} = \mathbf{C}\Gamma \quad (3)$$

where

$$\mathbf{q}^T = [\mathbf{q}_0 \mathbf{q}_S \mathbf{q}_A]^T = [q_1 q_2 \dots q_n \dots q_{n+3}]^T \\ = \left[ (\vartheta \varphi \psi) (q_1 \dots q_4 \gamma)_{j_S} (q_X q_Y \phi_X \phi_Y \phi_Z)_{j_A} \right]^T, \quad j_S = 1, \dots, N_S, \quad j_A = 1, \dots, N_A, \quad (4)$$

and  $\mathbf{I}$  is the unit matrix of dimension (3 x 3). Thus,  $\mathbf{B}$  is the symmetric  $(n+3) \times (n+3)$  matrix of elements of  $\mathbf{J}$ ,  $\mathbf{J}_\sim$  and  $\mathbf{A}_m$  and  $n$  is the number of generalised co-ordinates used in the modelling of all the elastic parts together. The individual elements,  $b_{k,l}$ , are given by  $\partial P / \partial q_{k,l}$  where  $P$  is the potential energy of the FS's elastic parts and  $q_{k,l}$  is the  $k^{\text{th}}$  generalised co-ordinate of the  $l^{\text{th}}$  flexible appendage. The potential energy,  $P$ , is given by:-

$$P(\mathbf{q}_\sim) = \sum_{j=1}^{N_S} P_{S_j}(q_S) + \sum_{i=1}^{N_A} P_{A_i}(q_A) \quad (5)$$

and once expressions for  $P_{S_j}$  and  $P_{A_i}$  have been obtained any coefficient,  $b_{k,l}$ , may be determined. For example, in the fourth equation (3), the corresponding row elements are  $0, \dots, 0, b_{4,4} = \frac{12b_{11}(b_{11} + b_{21})}{4b_{11} + 21b_{21}}, b_{4,5} = -\frac{6b_{11}b_{21}}{4b_{11} + 21b_{21}}, 0, \dots, 0$ .

Then any scalar component equation of (3) (or (1)) may be written down. For example, the second equation is:-

$$a_{\varphi\vartheta} \ddot{\vartheta} + a_{\varphi\varphi} \ddot{\varphi} + a_{\varphi\psi} \ddot{\psi} + \sum_{j_S=1}^{N_S} (a_{\varphi q_1} \ddot{q}_1 + a_{\varphi q_2} \ddot{q}_2 + \dots + a_{\varphi \gamma} \ddot{\gamma})_{j_S} \\ + \sum_{j_A=1}^{N_A} (a_{\varphi q_X} \ddot{q}_X + a_{\varphi q_Y} \ddot{q}_Y + a_{\varphi \phi_X} \ddot{\phi}_X + a_{\varphi \phi_Y} \ddot{\phi}_Y + a_{\varphi \phi_Z} \ddot{\phi}_Z)_{j_A} = \Gamma_\varphi$$



and the fourth 
$$a_{q1\vartheta}\ddot{\vartheta} + a_{q1\phi}\ddot{\phi} + a_{q1\zeta}\ddot{\psi} + a_{q1q1}\ddot{q}_1 + a_{q1q2}\ddot{q}_2 + \dots + a_{q1\gamma}\ddot{\gamma} + \dots + a_{q1\phi_z}\ddot{\phi}_z + b_{q1q1}q_{11} + b_{q1q2}q_{21} = 0$$
 Thus, a

complete spacecraft model may be formed. Expressions for the remaining coefficients are not given here due to space limitations.

It should be noted that for space structures with a symmetrical configuration, the matrix  $\mathbf{A}$  is symmetric, and the work of deriving the coefficients may be nearly halved by using the relation  $a_{qi qj} = a_{qj qi}$ .

The foregoing caters for an arbitrary disposition of the flexible components with respect to the principal axes of the rigid centre-body and this is determined by the set of cross-coupling coefficients  $(a_{\vartheta\phi}, a_{\vartheta\psi}, a_{\psi\phi})$ . These, however, are very small in some practical cases where the spacecraft configuration is fairly symmetrical. The following simplified spacecraft model, obtained by setting the cross-coupling coefficients to zero, is then applicable:-

$$\begin{cases} J_{\alpha} \ddot{\alpha} + \sum_{i=1}^M a_{i\alpha} \ddot{q}_{i\alpha} = \Gamma_{\alpha}, & \alpha = \vartheta, \varphi, \psi \\ a_{j\alpha} \ddot{\alpha} + \sum_{i=1}^M J_{i\alpha} \ddot{q}_{i\alpha} + b_{i\alpha} q_{i\alpha} = 0, & j = 1, \dots, M \end{cases} \quad (6)$$

where  $\alpha$  is one of the three spacecraft attitude angles,  $\vartheta, \varphi, \psi$ , about the three centre-body principal axes, valid for small rotations of the spacecraft about a zero-attitude reference,  $q_{i\alpha}$  are the generalised co-ordinates of the flexural motion in the plane perpendicular to the rotation axis for  $\alpha$  and the constant coefficients of equations (6) are the elements of the matrixes  $\mathbf{J}$ ,  $\mathbf{J}^{-1}$ ,  $\mathbf{A}_m$ ,  $\mathbf{B}$ . This model has  $M$  flexure modes per axis and, of course, three rigid-body modes and since each of these modes is of second order, the complete model is of order,  $n = 6(M + 1)$ . This will be the highest order model available, model order reduction being applied before the control system synthesis is carried out. The original model will then be useful in carrying out simulation studies to explore the effects of ignoring some of the modes in particular cases.

### 3 The Modal Physical Model

In the three-axis de-coupled LFS model (6) the attitude co-ordinates,  $\alpha = \vartheta, \varphi, \psi$ , are those of the rigid centre-body which may be assumed directly measurable. This may be represented as a sum of two basic components:-

$$\alpha = \bar{\alpha} + \tilde{\alpha} = \bar{\alpha} + \sum_{i=1}^M \tilde{\alpha}_i \quad (7)$$



where  $\bar{\alpha}$  is the attitude angle that would result from the same control torques applied to a rigid-body spacecraft with the same total moments of inertia as the complete LFS and  $\tilde{\alpha} = \sum_{i=1}^M \tilde{\alpha}_i$  is the component of the true spacecraft attitude co-ordinate due solely to the elastic oscillations.

The general co-ordinates,  $q_{i\alpha}$ , of model (6) cannot be identified in the physical system. For the purpose of designing an attitude control law, it would be better to obtain a model in which the co-ordinates are either physically measurable those associated with the flexure mode dynamics being directly related to the elastic mode displacements. In view of this, the resulting model will be referred to as the *modal physical model*. To this end, equations (6) will be expressed in terms of  $\bar{\alpha}$  and  $\tilde{\alpha}_i$ . The most straightforward way of achieving this is to convert equations (6) to the Laplace transfer function form and solve them with respect to  $\alpha(s) = \mathcal{L}\{\alpha(t)\}$ . This will be of the form:-

$$W_{\alpha}(s) = \frac{\alpha(s)}{f_{\alpha}(s)} = \frac{D(s)}{s^2 C(s)} \quad (8)$$

where  $f_{\alpha} = \Gamma_{\alpha}/J_{\alpha}$  will be defined as the control acceleration and,

$$C(s) = c_{2M}s^{2M} + c_{(2M-1)}s^{(2M-1)} + \dots + c_2s^2 + c_0, \quad D(s) = d_{2M}s^{2M} + d_{(2M-1)}s^{(2M-1)} + \dots + d_2s^2 + d_0$$

where  $c_k, d_k$  are constant coefficients depending on the mechanical and geometric parameters of the LFS configuration. This approach to modelling has been pursued by Rutkovsky and Suhkanov[8]. The double integrator factor of transfer function (8) results from the fact that the spacecraft rotates in space only under the influence of the control torques and without any damping torques from the surrounding medium which is assumed to be a vacuum. It should also be noted that only even powers of  $s$  appear in the polynomials,  $C(s)$  and  $D(s)$  because zero natural damping is assumed in the spacecraft structure on the basis that in practice they are known to be of the order of  $10^{-3}$  which is negligible. Transfer function (8) may now be written as:-

$$W_{\alpha}(s) = \frac{\bar{\alpha}(s)}{f_{\alpha}(s)} + \frac{\tilde{\alpha}(s)}{f_{\alpha}(s)} = W_{\bar{\alpha}}(s) + W_{\tilde{\alpha}}(s) = \frac{D(s)}{s^2 C(s)} \quad (9)$$

where  $W_{\bar{\alpha}}(s) = \bar{\alpha}(s)/f_{\alpha}(s)$  is the transfer function of the LFS as a rigid body, and  $W_{\tilde{\alpha}}(s) = \tilde{\alpha}(s)/f_{\alpha}(s)$  is the transfer function representing the oscillatory component of the spacecraft motion. Partial fraction expansion of the right

hand side of transfer function (9) yields  $\frac{D(s)}{s^2 C(s)} = \frac{d_0}{c_0 s^2} + H(s)$  where,

$\frac{d_0}{c_0 s^2} = \frac{\bar{\alpha}(s)}{f_\alpha(s)}$  on the basis that the rigid-body motional response to the control torque must be that of a double integrator. It then follows that  $H(s) = W_{\bar{\alpha}}(s)$  comprises the remaining terms of the partial fraction expansion which model the flexure mode dynamics. Setting  $c_0 = d_0$  without loss of generality then yields, upon comparison with equation (9):-

$$\begin{aligned}
 W_{\bar{\alpha}}(s) &= \frac{\tilde{\alpha}(s)}{f_\alpha(s)} = W_\alpha(s) - W_{\bar{\alpha}}(s) = \frac{D(s) - C(s)}{s^2 C(s)} \quad (10) \\
 &= \frac{(d_{2M} - c_{2M})s^{2(M-1)} + (d_{2(M-1)} - c_{2(M-1)})s^{2(M-2)} + \dots + (d_2 - c_2)}{c_{2M}s^{2M} + c_{2(M-1)}s^{2(M-1)} + \dots + c_2s^2 + c_0}
 \end{aligned}$$

Since the polynomial,  $C(s)$ , contains only even powers of  $s$ , the remaining terms of the partial fraction expansion must be of the form,  $\tilde{k}_i / (s^2 + \omega_i^2)$  and these may be recognised as simple harmonic oscillators with natural frequencies,  $\omega_i$ , as would be expected in the flexure mode part of the model. These terms may then be associated on a one-to-one basis with the individual flexural motion variables,  $\tilde{\alpha}_i$ . Then, recalling that  $\tilde{\alpha} = \sum_{i=1}^M \tilde{\alpha}_i$  :-

$$W_{\bar{\alpha}}(s) = \frac{\tilde{\alpha}(s)}{f_\alpha(s)} = \frac{\sum_{i=1}^M \tilde{\alpha}_i}{f_\alpha} = \sum_{i=1}^M W_{\alpha_i} = \sum_{i=1}^M \frac{\tilde{k}_i}{(s^2 + \omega_i^2)} = \frac{\sum_{i=1}^M \left[ \tilde{k}_i \prod_{i=1, i \neq j}^M (s^2 + \omega_i^2) \right]}{\prod_{i=1}^M (s^2 + \omega_i^2)} \quad (11)$$

Comparing the right hand sides of equations (10) and (11) then yields the following system of  $2m$  simultaneous equations in  $\tilde{k}_i$  and  $\omega_i^2$  :-

$$\left\{ \begin{aligned}
 \sum_{i=1}^M \tilde{k}_i &= d_{2M} - c_{2n} = \frac{J_{\sim}}{J_0}, & \sum_{j=1}^M \left( \tilde{k}_j \sum_{i=1, i \neq j}^M \omega_i^2 \right) &= d_{2(M-1)} - c_{2(M-1)}, \\
 & \dots & \sum_{j=1}^M \left( \tilde{k}_j \prod_{i=1, i \neq j}^M \omega_i^2 \right) &= d_2 - c_2
 \end{aligned} \right. \quad (12a)$$

$$\sum_{i=1}^M \omega_i^2 = c_{2(M-1)}, \quad \sum_{i=1, i \neq j}^M \omega_i^2 \omega_j^2 = c_{2(M-2)}, \dots, \prod_{i=1}^M \omega_i^2 = c_0 \quad (12b)$$



Assuming that the coefficients,  $c_i$ , are known in the first place, equations (12b) may be solved for  $\tilde{\omega}_i^2$ . Then equations (12a) may be solved for the coefficients  $\tilde{k}_i$ . It is evident from equation (11) that these coefficients determine the relative amplitudes of the oscillations of each mode caused by a given arbitrary input,  $m_\alpha(t)$ . They are therefore referred to as the *excitability coefficients* defined by Rutkovsky and Sukhanov[9]. Finally, transforming the transfer functions,  $W_{\tilde{\alpha}}(s)$  and  $W_{\tilde{\alpha}}(s)$ , to the time domain yields the following differential equations of the modal physical model:-

$$\ddot{\tilde{\alpha}} = f(u_\alpha), \quad f(u_\alpha) = \Gamma_\alpha(u_\alpha)/J_\alpha \quad (13a)$$

$$\ddot{\tilde{\alpha}}_i + \tilde{\omega}_i^2 \tilde{\alpha}_i = \tilde{k}_i f(u_\alpha), \quad i = 1, \dots, M \quad (13b)$$

$$\tilde{\alpha} = \sum_{i=1}^M \tilde{\alpha}_i, \quad \alpha = \bar{\alpha} + \tilde{\alpha} \quad \alpha = \varphi, \vartheta, \psi \quad (13c)$$

where  $u_\alpha$  is the input to the control actuator determined by a suitable control law,  $u_\alpha = u_\alpha(\alpha, \dot{\alpha}, t)$ . The function  $\Gamma_\alpha(u_\alpha)$ , represents the actuator transfer characteristic. Given the structure of the modal physical model, then the vector of ordered fundamental frequencies  $\tilde{\omega} = (\tilde{\omega}_1 < \tilde{\omega}_2 < \dots < \tilde{\omega}_M)$  and the corresponding vector of excitability coefficients  $\tilde{k} = (\tilde{k}_1, \tilde{k}_2, \dots, \tilde{k}_M)$  together determine the dynamic characteristics of the spacecraft.

#### 4 The Dynamic Portrait

The new theory of the dynamic portrait will now be presented. Let a structural design parameter of the spacecraft, such as the length of a solar panel be denoted by  $\lambda$ . Then the spacecraft dynamic parameters,  $\omega_i$  and  $\tilde{k}_i$ , in model (13) will be functions of  $\lambda$ , i.e.,  $\tilde{\omega}_i^2(\lambda)$  and  $\tilde{k}_i(\lambda)$ . Another important parameter is the mean value of the flexure mode displacement with a constant control acceleration of magnitude,  $f_\alpha$ , and this will also be a function of  $\lambda$ . From equation (13b), this is seen to be:-

$$\tilde{\alpha}_{c_i}(\lambda) = \frac{f_\alpha \tilde{k}_i(\lambda)}{\tilde{\omega}_i^2(\lambda)}, \quad i = 1, 2, \dots, M \quad (14)$$

This, in effect, is another form of modal excitability parameter with a larger emphasis on low frequency modes than the previously defined modal excitability coefficient,  $\tilde{k}_i(\lambda)$ . In general, the graph of the  $j^{\text{th}}$  dynamic parameter,  $P_j$  as a

function of the  $k^{\text{th}}$  structural parameter,  $\lambda_k$ , may be plotted to form a family of characteristics,  $P_j(\lambda_k)$ ,  $j \in (1, J)$ ,  $k \in (1, K)$  and this provides what may be referred to as the *dynamic portrait*[9] of the spacecraft. An example of such a dynamic portrait is shown in Figure 5.

As pointed out previously, a model should first be developed representing the real spacecraft. This should be as accurate as possible, including *all* the modes that are suspected of having even the slightest interaction with the attitude control loops to be designed. This model, however, will inevitably be of a considerably high order, perhaps several hundred in some cases, and it is therefore desirable to obtain a realistic model of lower order containing only the modes requiring active damping. It commonly believed that the most dominant modes are always the lowest frequency ones, leading to the simple model order reduction method of eliminating all the modes above a certain frequency. For any ordered pair of natural frequencies,  $\tilde{\omega}_i < \tilde{\omega}_{i+1}$ , it is possible, however, to have  $\tilde{\alpha}_{c1} > \text{or} < \tilde{\alpha}_{c2}$ . Thus, *the most dominant mode is not necessarily the lowest frequency one*, but certainly has the highest value of  $\tilde{\alpha}_c$  which will be denoted by  $\tilde{\alpha}_{cd}$ . This leads to the more rigorous model order reduction method of ranking the modes with respect to the relative degrees of modal excitability,  $\tilde{\alpha}_{ci}$  and eliminating all the modes having values below a chosen threshold. Unfortunately, there is no available formula for the choice of this threshold and it is therefore a matter of judgement. It is suggested here, however, that any mode for which

$$\tilde{\alpha}_{ci} \leq 0.1\tilde{\alpha}_{cd} \quad (15)$$

may be ignored. The dynamic portrait is envisaged to be a useful tool in this model reduction process, using, for example, the third family of characteristics in Figure 5.

At the opposite end of the scale, it is interesting to note that some structures exist, with particular reference to the branched mechanical configuration, in which one or more flexure modes are not substantially excited by the control actuators. In theory, *uncontrollable* modes are possible in the sense that  $\tilde{\alpha}_{ci} = 0$ . This condition may easily be determined with the aid of the dynamic portrait by searching for minima of  $\tilde{\alpha}_{ci}(\lambda)$  with respect to  $\lambda$ . Such uncontrollable modes are evident Figure 5. This leads to the concept of designing a spacecraft structure to purposely satisfy this condition for as many flexure modes as possible to minimise the number of significant modes requiring active control, but this must be done with extreme caution, paying attention to sources of external disturbance that may excite the uncontrollable modes through acting on different regions of the structure than the rigid centre-body

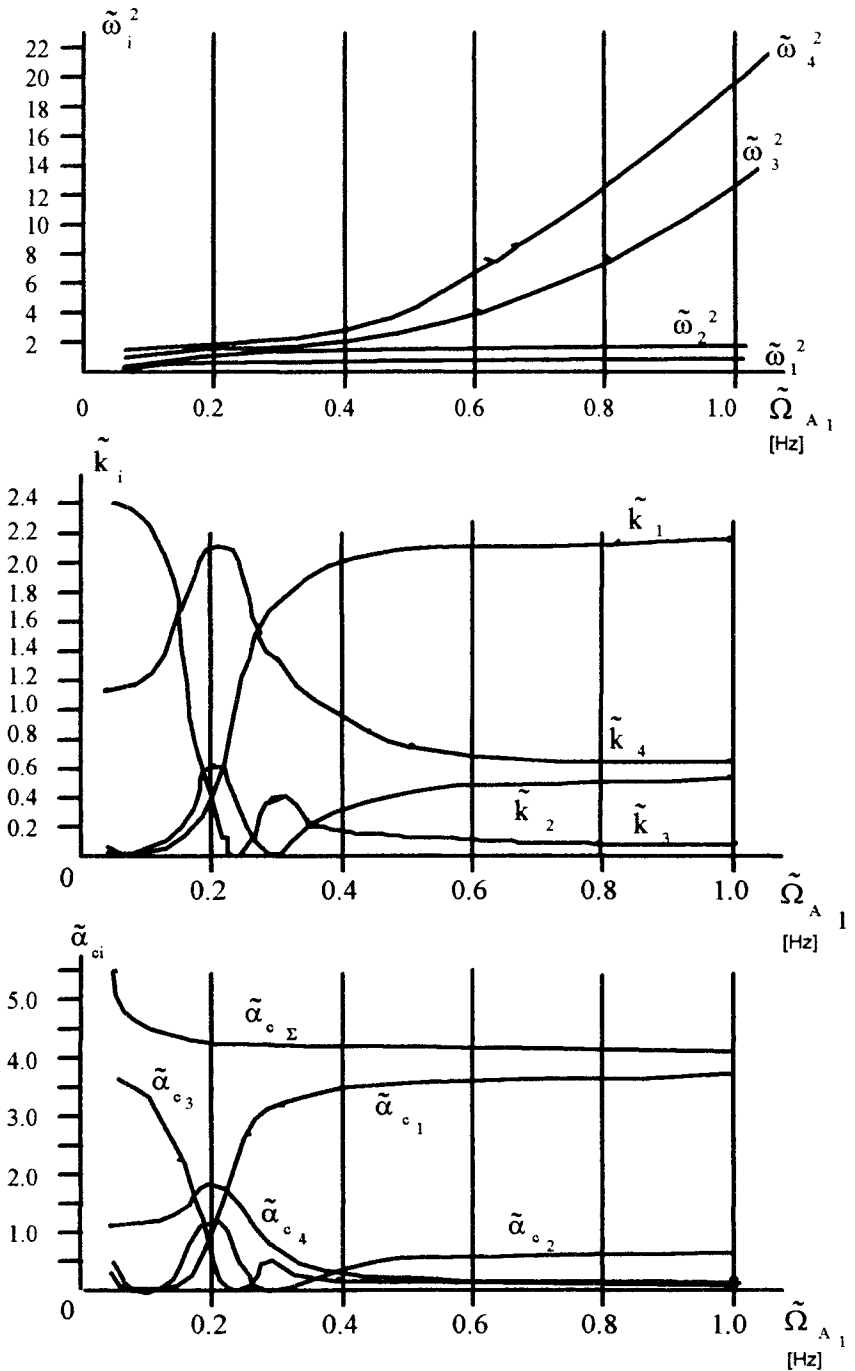


Figure 5 An example of a dynamic portrait



where the control actuators are situated.

In view of the foregoing, the reduced order model for control system synthesis comprises equation (13a) of the rigid centre-body together with  $m$  of the  $M$  flexure mode equations (13b) which must be taken into consideration in compliance with condition (15). The lowest order LFS model comprises the rigid-body part of equation (13a) together with just the dominant flexure mode,  $\tilde{\alpha}_d$ . It is suggested that after the model order reduction has been carried out that the original model is retained for inclusion in control system simulations to confirm the validity of the simplified model on which the control law is based.

The following section develops another analysis method appropriate to attitude control systems employing on-off gas jet actuators, again using the modal physical model (13).

## 5 Double Phase Plane Analysis of LSS

### 5.1 The Basic Trajectories

This alternative method of analysis of FS and particularly LFS, leading to model order reduction, is that of the double phase plane (DPP) of Rutkovsky and Sukhanov[2][3] and is particularly useful where gas-jet (on-off thruster) control actuators are employed with special control laws intended to achieve active modal damping such as generated by Dodds and Williamson[10] and Rutkovsky and Sukhanov[11]. The method is based on the well known phase plane method for second order systems. Each of the co-ordinates of the modal physical model is described by a second order sub-system and, as previously stated, is influenced only by the control variables and not by other co-ordinates. After expressing each of these sub-systems in the control canonical form, therefore, their phase-trajectories may be plotted on individual phase planes. Here, phase variables are defined as state variables of a chain of pure integrators, comprising the output of the last integrator and its time derivatives, as in the control canonical form.

The essence of the DPP method is to first plot the rigid-body phase trajectory  $[\bar{\alpha}(t), \dot{\bar{\alpha}}(t)]$  and then plot the modal phase trajectories  $[\tilde{\alpha}_i(t), \dot{\tilde{\alpha}}_i(t)]$  on the same diagram but with all their origins moved to the point,  $[\bar{\alpha}(t), \dot{\bar{\alpha}}(t)]$ . In this way the effect of individual flexure modes on the attitude motion of the spacecraft may be displayed on a single diagram by superimposing the phase trajectory of the flexure mode in question on the rigid-body phase trajectory. In this process, of course, the axes of the flexure mode phase plane remain parallel to but translate with respect to the fixed axes of the rigid-body phase plane.

In order to carry out the double phase plane analysis, the aforementioned phase trajectories will be determined analytically. First, the following scaling of



the modal rates is carried out to ensure that the phase trajectory of the dominant flexure mode is circular with a constant control variable. Thus:-

$$\bar{\beta} = \frac{\dot{\bar{\alpha}}}{\tilde{\omega}_d}, \quad \tilde{\beta} = \frac{\dot{\tilde{\alpha}}}{\tilde{\omega}_d}$$

The same scaling is applied to both rates to enable a direct comparison between the rigid body and flexure mode motions to be made. The rigid-body and dominant flexure mode state differential equations corresponding to equations (13a) and (13b) are then, respectively:-

$$\left\{ \begin{array}{l} \dot{\bar{\alpha}} = \tilde{\omega}_d \bar{\beta} \\ \dot{\bar{\beta}} = \frac{1}{\tilde{\omega}_d} m(u) = \frac{\tilde{\omega}_d}{k_d} \alpha_c(u) \end{array} \right. \quad \text{and} \quad \left\{ \begin{array}{l} \dot{\tilde{\alpha}} = \tilde{\omega}_d \tilde{\beta} \\ \dot{\tilde{\beta}} = -\tilde{\omega}_d \tilde{\alpha} + \frac{\tilde{k}_d}{\tilde{\omega}_d} m(u) = -\tilde{\omega}_d \tilde{\alpha} + \tilde{\omega}_d \tilde{\alpha}_c(u) \end{array} \right.$$

noting from equation (14) that  $m(u) = \frac{\tilde{\omega}_d^2}{k_d} \tilde{\alpha}_c(u)$ . Dividing the left hand sides

of these equations to eliminate time then yields the corresponding *phase trajectory differential equations*:-

$$\frac{d\bar{\alpha}}{d\bar{\beta}} = \tilde{k}_d \frac{\bar{\beta}}{\alpha_c(u)}, \quad \frac{d\tilde{\alpha}}{d\tilde{\beta}} = \frac{\tilde{\beta}}{\tilde{\alpha} + \tilde{\alpha}_c(u)}$$

In the case of gas-jet control,  $m(u(t))$  is a piecewise constant function and these equations may be solved by the method of separation of variables. Thus:-

$$\bar{\alpha} = \bar{\alpha}_0 + \frac{k_d(\bar{\beta}^2 - \bar{\beta}_0^2)}{2\tilde{\alpha}_c(u)} \quad (16)$$

$$\tilde{\beta}^2 + [\tilde{\alpha} - \tilde{\alpha}_c(u)]^2 = \tilde{\beta}_0^2 + [\tilde{\alpha}_0 - \tilde{\alpha}_c(u)]^2 \quad (17)$$

where  $\bar{\alpha}_0$ ,  $\bar{\beta}_0$ ,  $\tilde{\alpha}_0$  and  $\tilde{\beta}_0$  are the initial phase variables. It is evident from equations (16) that the phase portrait of the rigid-body mode is a family of parabolic trajectories symmetrical about the  $\tilde{\alpha}$  axis and that the phase portrait of the dominant flexure mode is a family of circular trajectories with centre at the point,  $[\tilde{\alpha}_c(u), 0]$ . In the polar co-ordinate system, these trajectories can be represented by a radius vector,  $\rho$ , of length equal to the amplitude of oscillations relative to the static deflection,  $\tilde{\alpha}_c$ . Thus:-

$$\rho = (\tilde{\beta}^2 + [\tilde{\alpha} - \tilde{\alpha}_c(u)]^2)^{\frac{1}{2}} \quad (18)$$

The oscillation phase,  $\phi$ , measured as the clockwise increasing angle between the line of length,  $r$ , joining the point,  $[\bar{\alpha}(t), \dot{\bar{\alpha}}(t)]$  to the describing point,  $[\tilde{\alpha}(t) + \tilde{\alpha}(t), \dot{\tilde{\alpha}}(t) + \dot{\tilde{\alpha}}(t)]$  of the true attitude motion is given by:-

$$\phi = \text{arctg} \left( \frac{\tilde{\beta}}{\tilde{\alpha} - \tilde{\alpha}_c(u)} \right) \quad (19)$$

The trajectories discussed above are illustrated in Figure 6.

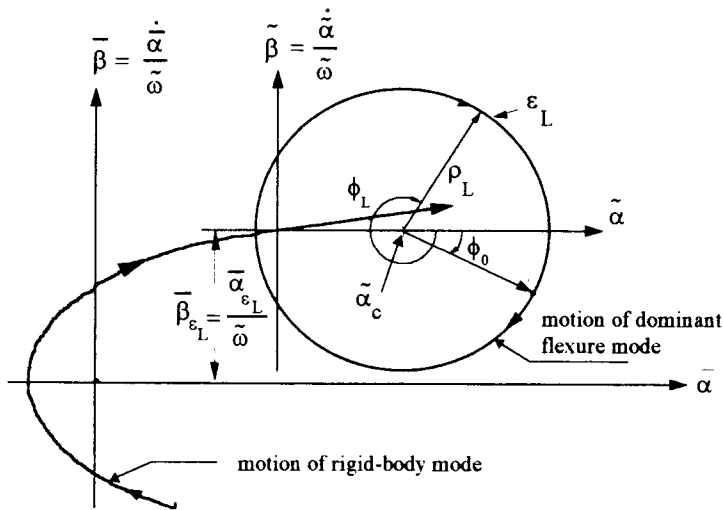


Figure 6 Double phase plane diagram for rigid body mode and dominant flexure mode alone and constant control torque

The complete phase trajectories, of course, depend on the timing of the sequence of piece-wise constant control torques produced by the particular gas-jet control law employed but the trajectories described in this section may be used to analyse the system for each interval of constant  $u$ .

## 5.2 Wash-out Double Phase Plane

For spacecraft models with more than one flexure mode, the double phase plane method introduced in section 4.1 may be extended to display the attitude motion of the spacecraft on a single diagram by adding the individual flexure mode

displacements and similarly adding the flexure mode rates to form a composite flexure mode phase trajectory which, after several cycles of the lowest frequency component have passed, appears as a “noisy” ring instead of a circle. In the phase double plane, this trajectory is superimposed on the parabolic rigid-body phase trajectory, sweeping out a swathe on the diagram which appears as a ‘noisy ring’, as illustrated in Figure 7.

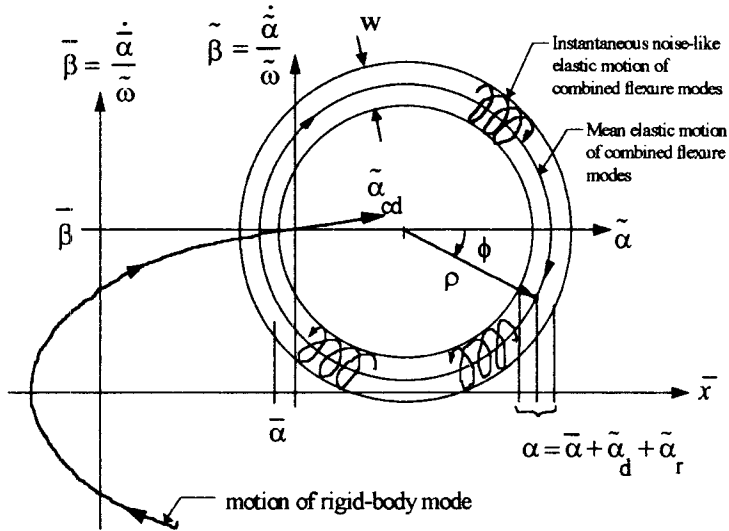


Figure 7 Double phase plane diagram for rigid body mode and multiple flexure modes and constant control torque

This effect gives rise to the name ‘wash-out double phase plane’. The statistical mean radius,  $\rho$ , of the noisy ring forms a useful means of assessing the overall effect of the flexure mode oscillations. This can be calculated as follows. Let

$$\chi = \frac{\sum_{i=1, i \neq d}^M \tilde{\alpha}_{ci}}{\tilde{\alpha}_{cd}} = \frac{\tilde{\alpha}_{c\Sigma}}{\tilde{\alpha}_{cd}} - 1 \quad (20)$$

where  $\tilde{\alpha}_{c\Sigma} = \sum_{i=1}^M \tilde{\alpha}_{ci} = \sum_{j=1}^J \frac{\tilde{b}_j}{J} b_j^{-1}$  is defined as the degree of excitability of the multiple-frequency elastic oscillations and  $b_j$  is the coefficient of reduced rigidity of the  $i^{\text{th}}$  elastic link. Then the width of the noisy ring is given by:-

$$w = \chi \tilde{\alpha}_{cd}$$

An interesting approach of Rutkovsky and Sukhanov[12] is to simplify the flexure mode model by starting with just the circular trajectory,  $[\alpha(t), \beta(t)]$ , of

the dominant flexure mode superimposed on the parabolic rigid-body mode trajectory, yielding a similar double phase plane trajectory to that shown in Figure 6. Then, the remaining  $M-1$  modes are replaced by an equivalent narrow-band random process. This is a *single* sinusoid:-

$$\alpha_r(t) = A_r(t) \cos[\omega_r(t) + \phi_r(t)] \quad (21)$$

where  $A_r(t)$ ,  $\omega_r(t)$  and  $\phi_r(t)$  are, respectively, the amplitude, frequency and phase which are each *random variables* with probability distributions chosen to closely approximate the sum of the  $M$  sinusoidal components of the real flexure modes with constant amplitudes, frequencies and phase angles. The trajectory,  $[\alpha_r(t), \beta_r(t)]$  of this random process, where  $\beta_r(t) = \dot{\alpha}_r(t)$ , is then superimposed on the determinate circular trajectory  $[\tilde{\alpha}_d(t), \tilde{\beta}_d(t)]$  of the dominant mode to yield a double phase plane diagram as in Figure 7.

## 6 Precise Definition of Large Flexible Spacecraft

The modal physical model and the double phase plane method will now be used to introduce quantitative correlations providing an exact definition of large flexible spacecraft.

Once the parameters of model (13) are assigned, then the spectrum boundaries of the fundamental frequencies of the elastic oscillations may be calculated. The lower bound coincides with the magnitude of the mode with the lowest frequency,  $\tilde{\omega}_1$ . Then, the closeness of the upper bound of the closed-loop attitude control system frequency response, assuming rigid-body dynamics, to  $\tilde{\omega}_1$  determines the degree of difficulty in guaranteeing the stability of both the rigid-body motion and the flexural motion, as pointed out by Nurr et. al.[1], thereby determining the complexity of the control law ultimately to be applied in terms of the number of flexure modes that must be actively controlled together with the rigid-body mode. The synthesis of suitable control laws has occupied researchers for many years, particularly for gas-jet control where several innovative methods have emerged, such as generated by Rutkovsky and Sukhanov[2] and Dodds and Williamson [10].

The significance of a given flexure mode in the modal physical model may be assessed by comparing its motion with that of the rigid-body mode, considering deviations about the desired steady-state condition of the spacecraft which, in most cases is zero flexure mode state and zero centre-body pointing error. A simply way of achieving this is to set zero initial state variables of the model, corresponding to the desired state and then apply a constant control torque and compare the modal states. The differential equations of motion



(13a) and (13b) for  $f_\alpha(u) = \text{const}$ , and zero initial conditions  $\bar{\alpha}_0 = \dot{\bar{\alpha}}_0 = \tilde{\alpha}_0 = \dot{\tilde{\alpha}}_0 = 0$  have the following solutions, considering just one mode and omitting the suffix, i, for simplicity of notation:-

$$\dot{\bar{\alpha}}(t) = f_\alpha t, \quad \bar{\alpha}(t) = \frac{1}{2} f_\alpha t^2 \quad (22)$$

$$\dot{\tilde{\alpha}}(t) = \tilde{\omega} \tilde{\alpha}_c \sin(\tilde{\omega} t), \quad \tilde{\alpha}(t) = \tilde{\alpha}_c [1 - \cos(\tilde{\omega} t)] \quad (23)$$

where  $\tilde{\alpha}_c = f_\alpha \tilde{k} \tilde{\omega}^{-2}$ . Figure 8 shows a sketch of these solutions for three different values of the modal excitability coefficient,  $\tilde{k}$ .

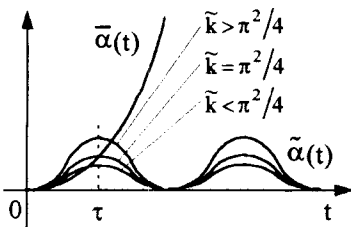


Figure 8 Comparison of rigid-body and flexure mode displacements

The first maximum of  $\tilde{\alpha}(t)$  may be either greater or less than  $\bar{\alpha}(t)$  at time  $t = \tau$ . Clearly, for rigid body like behaviour,  $\tilde{\alpha}(\tau) < \bar{\alpha}(\tau)$  and for  $\tilde{\alpha}(\tau) > \bar{\alpha}(\tau)$ , the flexure mode is very significant. The intermediate condition,  $\tilde{\alpha}(\tau) = \bar{\alpha}(\tau)$ , may therefore be used to define a boundary separating large flexible spacecraft from others. Hence, a spacecraft falls within the LFS class if

$$\tilde{\alpha}(\tau) \geq \bar{\alpha}(\tau) \quad (24)$$

According to the second of equations (23), the flexure mode displacement first reaches its maximum value at half the modal period. Hence  $\tau = \pi / \tilde{\omega}$ . Evaluating  $\bar{\alpha}(\tau)$  and  $\tilde{\alpha}(\tau)$  using the second of equations (22) and (23) then

yields  $\bar{\alpha}(\tau) = \frac{1}{2} f_\alpha \frac{\pi^2}{\tilde{\omega}^2}$  and  $\tilde{\alpha}(\tau) = 2f_\alpha \frac{\tilde{k}}{\tilde{\omega}^2}$  and so condition (24) is equivalent

to the following condition that an LFS must satisfy:-

A spacecraft is an LFS if  $\tilde{k} \geq \frac{\pi^2}{4}$  for any flexure mode

(25)

Since this definition is independent of the flexure mode frequency, however, it cannot be used alone to define a boundary segregating the class of LFS from the others. Spacecraft not qualifying as LFS would be expected to exhibit dynamic behaviour resembling that of a rigid body. It is possible for a spacecraft with a very low frequency flexure mode and low excitability coefficient, which hardly approximates a rigid body, to satisfy definition (25). It will therefore be considered only as a necessary condition for LSS. Hence a further criterion

will now be sought which involves the flexure mode frequencies to complete the definition of LFS. Phase plane analysis will be employed for this purpose, with the same zero initial conditions as before.

The focus of the parabolic phase plane trajectory

$$\dot{\bar{\alpha}}^2 = 2f_{\alpha} \bar{\alpha} \quad (26)$$

of the rigid-body mode is located on the  $\bar{\alpha}$  axis at the point  $(\bar{\alpha}, \dot{\bar{\alpha}}) = (0.5f_x, 0)$ , as indicated in Figure 9. Since the lower bound of the elastic mode spectrum is

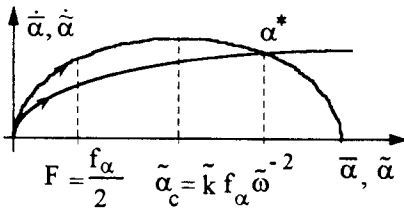


Figure 9 Comparison of rigid body and lowest frequency flexure mode phase trajectories

defined by the frequency,  $\tilde{\omega}_1$ , of the first mode, only this mode will be considered. Its trajectory in the phase plane is an ellipse

$$\dot{\tilde{\alpha}}^2 \tilde{\omega}^{-2} + [\tilde{\alpha} - \tilde{\alpha}_c]^2 = \tilde{\alpha}_c^2 \quad (27)$$

with centre at the point,  $(\tilde{\alpha}, \dot{\tilde{\alpha}}) = (f_{\alpha} \tilde{k} \tilde{\omega}^{-2}, 0)$ . Figure 8 shows that there is a point of intersection of the two trajectories at  $\bar{\alpha} = \tilde{\alpha} = \alpha^*$ . The

rigid-body mode trajectory (26) is determined by only one parameter,  $F = f_{\alpha}/2$ , and is therefore 'frozen' by setting  $f_{\alpha} = \text{const}$ . On the other hand, the eccentricity and centre of the elliptical flexure mode trajectory (27) may be changed, respectively, by means of  $\tilde{\omega}$  and  $\tilde{k}$ .

It should be noted that although the trajectories of Figure 9 cross at the point,  $\bar{\alpha} = \tilde{\alpha} = \alpha^*$ , in general, they do not pass through this point at the same time. The constraints imposed on the relative values of  $F$  and  $\tilde{\alpha}_c$  by coincident arrival at the point of coincidence in Figure 9 for different flexible spacecraft subject to the same control acceleration,  $f_x$ , will now be examined. The simultaneous solution of equations (26) and (27) forces arrival of the describing points of the trajectories at the point of intersection at the same time, yielding:-

$$\alpha^* = \frac{2f_{\alpha}}{\tilde{\omega}^2} (\tilde{k} - 1) \quad (28)$$

Hence, the coincidence is only possible if  $\tilde{k} > 1$ . It should be noted that the necessary condition (25) automatically satisfies this inequality. With this assumption, the variations of  $F$  and  $\tilde{\alpha}_c$  over a wide range of  $\tilde{\omega}$  will now be determined. Since  $f_{\alpha}(u) = \text{const}$ , the shape of the parabolic rigid-body mode phase trajectory (26) is independent of  $\tilde{\omega}$ . As supposed previously, as  $\tilde{\omega}$  is increased indefinitely, the dynamic behaviour of the spacecraft approaches that



of a rigid body. Under these circumstances,  $\tilde{\alpha}_c \ll F$  because  $F = f_\alpha/2$  and  $\tilde{\alpha}_c = f_\alpha \tilde{k} \tilde{\omega}^{-2}$  which is very small for large  $\tilde{\omega}$  and the intersection (28) of trajectories occurs on the interval  $\tilde{\alpha} < 2\tilde{\alpha}_c$ . When  $\tilde{\omega}$  is small, the spacecraft has very little rigidity and  $\tilde{\alpha}_c \gg F$  with the result that the elliptical flexure mode trajectory is stretched along the  $\tilde{\alpha}$  axis. In the region of intermediate magnitudes of  $\tilde{\omega}$ , the dynamic behaviour of the spacecraft is characterized by similar energy levels being associated with the components,  $\tilde{\alpha}$  and  $\tilde{\alpha}_c$ . In this case  $\tilde{\alpha}_c$  and  $F$  approach coincidence. In view of this, the condition  $\tilde{\alpha}_c \geq F$  together with condition (25) will be taken together as the final criterion for categorizing spacecraft as LFS. Since  $F = f_\alpha/2$  and  $\tilde{\alpha}_c = f_\alpha \tilde{k} \tilde{\omega}^{-2}$ , the condition,  $\tilde{\alpha}_c \geq F$ , is equivalent to:-

$$\tilde{\omega}^2 \leq 2\tilde{k} \quad (29)$$

The following definition of large flexible spacecraft may now be used instead of the less precise one given at the beginning of section 2.1.

*Any spacecraft of relatively large dimensions is a Large Flexible Spacecraft (LFS) if its dynamic behaviour is characterised in the modal physical representation by closeness of any of the flexure mode motions to the rigid-body motion, according to the conditions  $4\tilde{k}_i \geq \pi^2$  and  $\tilde{\omega}_i^2 \leq 2\tilde{k}_i$ ,  $i \in (1, \dots, M)$*

## 7 Conclusions and Recommendations for Further Research

A generic model of flexible spacecraft with a branched structure, comprising a rigid centre-body and flexible appendages has been presented together with a new definition of large flexible spacecraft, enabling a model of manageable order to be generated for the synthesis of attitude control systems. A new dynamic portrait has also been presented which is recommended for use in the structural design stage to facilitate the tailoring of the spacecraft dynamics to ease the application of a particular control strategy. An example is the minimisation of the excitability of flexural modes so that they may be ignored in the control system design, but this procedure would have to be followed with great care to ensure that external disturbances would not excite modes that are uncontrollable by via the control variables.

It is highly recommended that for the purpose of substantiating the new modelling methods presented, they are tried out with several different spacecraft and the application of various attitude control laws simulated, including those designed for on-off gas-jet actuators and continuous momentum exchange actuators such as reaction wheels and control moment gyros.





The new methods would be most effectively introduced as useful tools for practicing spacecraft control systems engineers by developing a user friendly computer aided design package in which they would be incorporated. Such a package would cater for the insertion of control laws under investigation to be inserted and realistic simulations to be carried out with the higher order spacecraft models used as the basis of the model order reduction.

## References

1. Nurr, G.S., Ryan, R.S., Scofield, H.N. and Sims J.L., Dynamics and Control of Large Space Structures, *Journal of Guidance, Control and Dynamics*, 1984, Vol.7, No.5, pp.514-526.
2. Rutkovsky, V.Yu. and Sukhanov, V.M., Phase Double-Plane as a Method to Study the Dynamics of Spacecraft with Limited Constructional Rigidity, *Proceedings of the 5-th World Congress IFAC*, Paris, 1972.
3. Rutkovsky, V.Yu. and Sukhanov, V.M., Investigation of flexible spacecraft elastic oscillations with the help of double-phase plane method, *Proceedings of scientific reading on cosmonautics, M.: Nauka*, 1979, p.152-159.
4. Kirk, C., (Editor) Dynamics and Control of Structures in Space II. *Proceedings of the Second International Conference on Dynamics and Control of Structures in Space*, Computational Mechanics Publications, Southampton Boston, 1993.
5. Lurye, A.I., Analytical mechanics, *M., phismatgiz*, 1961.
6. Likins, P.W., Dynamics and Control of Flexible Space Vehicles, *JPL*, 1970.
7. Nekhoroshiy Yu.I., Rutkovsky, V.Yu. and Sukhanov, V.M. Parameter Identification of Modal-Physical Model of Flexible Spacecraft, *Automation and Remote Control*, 1992, N7, pp.19-25.
8. Sukhanov V.M., Rutkovsky V.Yu., Motion Equations and Analysis of Flexible Spacecraft with Brached Structural Dynamics, Preprint, *M.:* *Institute of Control Sciences*, 1986.
9. Rutkovsky V.Yu. and Sukhanov V.M., The Model of Flexible Spacecraft and Main Characteristics of Structural Dynamics, *Technical Cybernetics*, 1994, N1, pp.198-206.
10. Dodds, S.J. and Williamson S.E., A Signed Switching Time Bang-Bang Attitude Control Law for Fine Pointing of Flexible Spacecraft, *Int.J.Control*, 1984, Vol.40, pp.795-811.
11. Rutkovsky, V.Yu. and Sukhanov, V.M., Attitude Control Algorithms in Flexible Satellites using Information on the Phase of Elastic Oscillations, *Proceedings of the 6-th IFAC Symposium on Automatic Control in Space*, USSR, 1974.
12. Rutkovsky V.Yu. and Sukhanov V.M., On the Predicting Properties of Flexible Spacecraft, *Proceedings of the 27-th Congress of the International Astronautical Federation, USA*, Pergamon Press, 1976.